

Spin-orbit Interaction induced Singlet-Triplet Resonant Raman Transitions in Quantum-dot Helium

Aram Manaselyan,¹ Areg Ghazaryan,¹ and Tapash Chakraborty²

¹*Department of Solid State Physics, Yerevan State University, Yerevan, Armenia*

²*Department of Physics and Astronomy, University of Manitoba, Winnipeg, Canada R3T 2N2*

From our theoretical studies of resonant Raman transitions in two-electron quantum dots (artificial helium atoms) we show that in this system, the singlet-triplet Raman transitions are allowed (in polarized configuration) only in the presence of spin-orbit interactions. With an increase of the applied magnetic field this transition dominates over the singlet-singlet and triplet-triplet transitions. This intriguing effect can therefore be utilized to tune Raman transitions as well as the spin-orbit coupling in few-electron quantum dots.

Quantum dots (QD) or the artificial atoms [1] containing two interacting electrons – popularly known as artificial helium atoms [2] have received considerable attention for over a decade because of their relative simplicity, but at the same time being rich in fundamental physics. One of the most interesting features in this system is the spin singlet-triplet transition in a externally applied magnetic field [3, 4]. This spin transition is a consequence of an interplay between the electron-electron interaction and the harmonic confinement potential [3]. It has been proposed that resonant Raman transitions [5, 6] are perhaps a direct route to observe this transition. We have studied Raman scattering in GaAs quantum dot helium for polarized configuration and we observed that in accordance with the experimental observations [5, 7, 8], due to the polarization selection rules, only singlet-singlet transitions are observed for zero magnetic field, while triplet-triplet transitions are possible for higher values of the magnetic field. In this Letter, we report that in the presence of the Rashba spin-orbit (SO) interaction [9], there are additional singlet-triplet and triplet-singlet Raman transitions that are forbidden without the SO interaction. Further, the external magnetic field can be used to tune the amplitudes of these new transitions.

A very useful mechanism for coherent spin manipulation in quantum nanostructures is via the Rashba SO interaction [9, 10] which couples the orbital motion of electrons with the spin state. The SO interaction can arise in a quantum dot due to the confinement and lack of inversion symmetry of the nanostructure which creates a local electric field perpendicular to the electron plane. The SO coupling strength can be varied by changing the asymmetry of the quantum structure with an external electric field. There were a few recent reports on the tunability of the SO interaction in few-electron quantum dots [11]. In our recent work on the Rashba effects in quantum dots [12, 13] we found multiple level crossings and level repulsions in the energy spectrum that was a result of the interesting interplay between the Zeeman effect and the SO interaction. The influence of Rashba and Dresselhaus SO interaction on the energy levels and optical absorption spectrum for two-electron QD was investi-

gated earlier [14]. We also found [15] that the Rashba SO coupling is responsible for additional Raman transitions, the amplitude of which can be controlled externally by changing the SO coupling parameter.

Following the experimental work of Singha et al. [7], we consider a GaAs/AlGaAs quantum dot with a diameter of 180 nm. We chose the confinement potential of the dot as parabolic with an oscillator energy $\hbar\omega_0$. The Hamiltonian of the N-electron system in the dot can be written as

$$\mathcal{H} = \sum_i^N \mathcal{H}_i^e + \frac{1}{2} \sum_{i,j}^N \frac{e^2}{\varepsilon |\mathbf{r}_i - \mathbf{r}_j|}, \quad (1)$$

where the second term describes the Coulomb interaction between electrons, e is the electron charge and \mathcal{H}_i^e is the single-electron Hamiltonian in the presence of an external perpendicular magnetic field and with the SO interaction included

$$\mathcal{H}_i^e = \frac{1}{2m_e} \Pi_i^2 + \frac{1}{2} m_e \omega_0^2 r_i^2 + \frac{1}{2} g \mu_B B \sigma_z + H_{\text{SO}}, \quad (2)$$

where $\Pi = \mathbf{p} - \frac{e}{c} \mathbf{A}$ and \mathbf{A} is the vector potential of the magnetic field. The third term on the right hand side of Eq. (2) is the Zeeman splitting. The last term describes the Rashba SO interaction [9]

$$H_{\text{SO}} = \frac{\alpha}{\hbar} \left[\boldsymbol{\sigma} \times \left(\mathbf{p} - \frac{e}{c} \mathbf{A} \right) \right]_z, \quad (3)$$

with α being the spin-orbit coupling constant, which is sample dependent and is proportional to the interface electric field that confines the electrons in the xy plane. In (2) and (3), $\boldsymbol{\sigma}$ is the electron spin operator and σ_x, σ_y and σ_z are the Pauli spin matrices. The eigenfunctions of the single-electron Hamiltonian (2) can be presented as a linear expansion of the Fock-Darwin orbitals [1] $f_{n,l}(r, \theta)$, where n, l are the radial and angular quantum numbers. The Rashba term H_{SO} in turn will couple the single-electron state with angular momentum l , and spin up to the state with angular momentum $l + 1$, and spin down [12]. The energy spectrum of the many-electron system was obtained by diagonalizing the Hamiltonian matrix (1).

In order to evaluate the Raman transition amplitudes, first we have to define the initial, final and the intermediate states. Let us consider the resonant inelastic light-scattering process in a backscattering configuration with the incident photon energy just above the effective band gap of the quantum dot and with the wave vector transfer in the lateral dimension $q = 2 \times 10^4 \text{cm}^{-1}$ [7]. In that case the initial states of the N-electron system will be the ground state, and the final states will be the intraband excitations of the N-electron system with the same total momentum projection J_z as for the initial state. For the intermediate states we have N+1 electrons in the conduction band and one additional hole in the valence band. For simplicity, we consider here only the heavy-hole states. Under this approximation the single-hole Hamiltonian and the wave functions are similar to those for the electron. We need to change only the values of the effective mass and the confinement parameter. It is well known that the Rashba effect on heavy hole ground state is very weak [13]. Hence we have neglected the SO effect on the hole states. The hole states can also be described with the help of the Fock-Darwin functions, and the basis functions of the intermediate states can be constructed as products of the Slater determinants of the electrons and the single-hole wave functions.

The Raman scattering transition amplitude from the initial state $|i\rangle$ to the final state $|f\rangle$ is obtained from [16]

$$A_{fi} \sim \sum_{\text{int}} \frac{\langle f|H^{(+)}|\text{int}\rangle \langle \text{int}|H^{(-)}|i\rangle}{\hbar\omega_i - (E_{\text{int}} - E_i) + i\Gamma_{\text{int}}}, \quad (4)$$

where $\hbar\omega_i$ is the incident photon energy. In equation (4) $H^{(-)}$ and $H^{(+)}$ are the single-particle operators describing the photon absorption (-) and emission (+) processes respectively [15, 16].

For Raman scattering, we need to consider two cases: (i) the polarized geometry, i.e., when the polarization vectors of incident and scattered photons are in the same direction, and (ii) the depolarized geometry, when the polarization vector of the scattered photon is perpendicular to that of the incident one.

The differential cross section of Raman scattering can be calculated using the following expression

$$d\sigma \sim \sum_f |A_{fi}|^2 \delta(\Delta E - (E_f - E_i)), \quad (5)$$

where $\Delta E = \hbar\omega_i - \hbar\omega_s$ is the Raman energy shift. In our calculations we have used a Lorentzian instead of the Dirac delta function in order to take into account the level width of the final states [15].

Energy levels – In our present study, we consider a GaAs QD with $m_e = 0.063m_0$, $m_h = 0.33m_0$, $\varepsilon = 12.9$ and we used uniform values for level widths $\Gamma_{\text{int}} = \Gamma_f = 0.5$ meV. In Fig. 1, the magnetic field dependence of the low-lying energy levels of a QD with one and two electrons is presented for different values of the total mo-

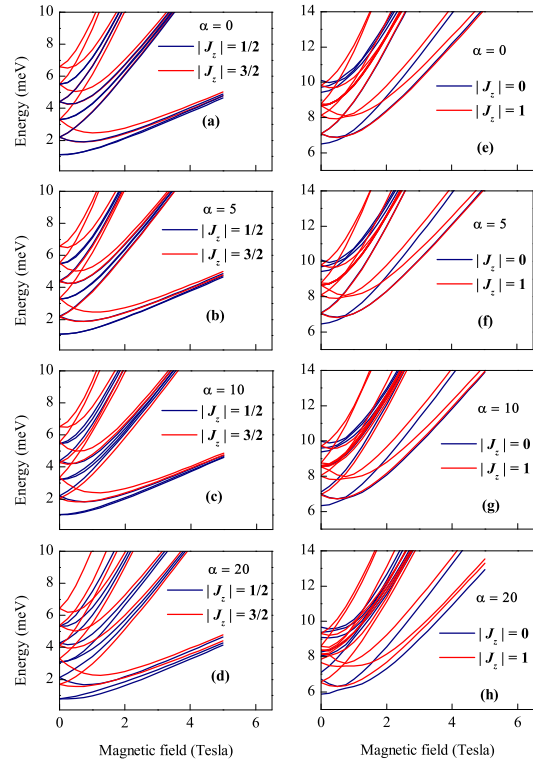


FIG. 1: Magnetic field dependence of the low-lying energy levels in a single-electron (a-d) and two-electron (e-h) quantum dot for various values of the SO coupling strength α (in meV nm).

mentum J_z and for four values of the SO coupling parameter $\alpha = 0, 5, 10, 20$ meV nm. This wide range of values of α provides a clear dependence of the energy spectra on this parameter. When compared with the Fock-Darwin spectra without the SO coupling (Fig. 1(a)), the most outstanding features in the energy spectra of the quantum dots with SO coupling are the lifting of degeneracy at a vanishing magnetic field, rearrangement of some of the levels at small fields, and the level repulsion at higher magnetic fields (Fig. 1(b) - (d)). For zero magnetic field and without the Rashba SO interaction, the ground state of a single-electron QD is characterized by $n = 0, l = 0, \sigma = \pm 1/2$ with the corresponding energy $\hbar\omega_0$. The next two excited states are $n = 0, l = \pm 1, \sigma = \pm 1/2$ and $n = 1, l = 0, \sigma = \pm 1/2$ with energies $2\hbar\omega_0$ and $3\hbar\omega_0$ respectively. The SO coupling in turn mixes the states $|l, 1/2\rangle$ with $|l + 1, -1/2\rangle$ and $|l, -1/2\rangle$ with $|l - 1, 1/2\rangle$, which removes the four-fold degeneracy for the first excited state and introduces some level repulsions at higher fields. Similar effects are clearly visible also for dots with two electrons (Fig. 1(e-h)). Therefore, with the SO coupling the total angular momentum and the total spin of the electrons are no longer good quantum numbers and we have to use the total momentum J_z instead, to describe the states [12, 13].

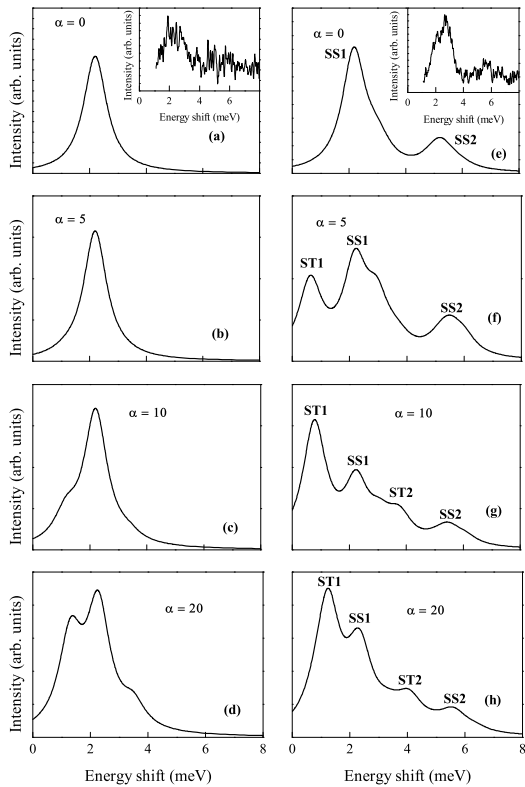


FIG. 2: The Raman scattering amplitudes for the polarized geometry and for various values of SO coupling parameter α (in meV nm) for single-electron (a-d) and for two-electron (e-h) quantum dot. Insets: Experimental data for $\alpha = 0$ from Ref. [7]

Raman spectra – The Rashba SO coupling can play an important role in Raman spectroscopy of the QDs. The effect of Rashba SO coupling on the Raman excitations for quantum dots containing one electron is shown in Fig. 2 (a-d) and for QDs with two electrons in Fig. 2(e-h). For a single-electron QD we considered the polarized Raman excitations between the states with total momentum $J_z = 1/2$ (blue lines in Fig. 1 (a-d)). For a two-electron QD we considered similar excitations between the states with total momentum $J_z = 0$ (blue lines in Fig. 1 (e-h)).

We begin with the Raman scattering for one and two electron quantum dots without the SO coupling (Fig. 2 (a) and (e)). The experimentally measured values of the resonant Raman scattering amplitudes for the polarized geometry are presented as insets of Fig. 2 for a dot with one and two electrons. The theoretical results are in good agreement with the experimental data [7]. It is easy to see from the experimental data that for the case of the one-electron QD, we have only one peak with the Raman energy shift of $\Delta E = 2.2$ meV. That peak corresponds to the excitation of the system from the ground state $|0,0\rangle$ to the first excited state with the same angular momentum $|1,0\rangle$ with energy difference $2\hbar\omega_0$. Therefore, we can use the value $\hbar\omega_0 = 1.1$ meV in our calculations

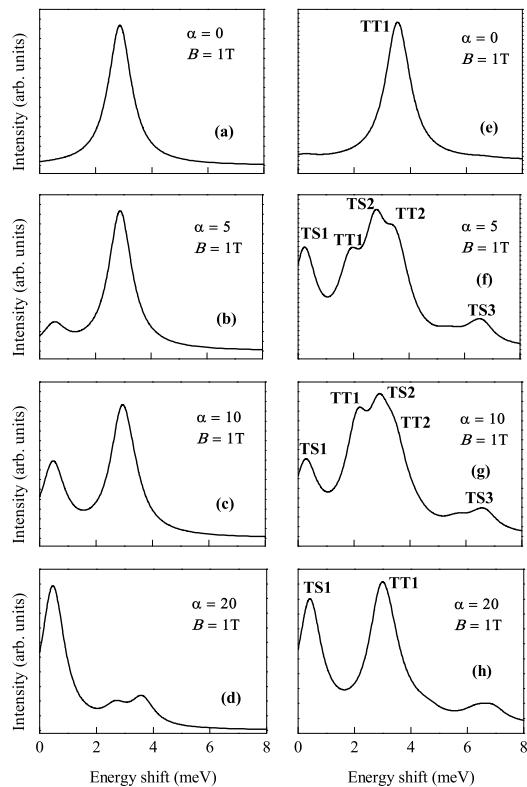


FIG. 3: The same as in Fig. 2, but for a magnetic field of 1 Tesla.

for the single-electron QD, and we use $\hbar\omega_h = 1$ meV for the hole. In the case of a quantum dot with two electrons (Fig. 2(e) and corresponding inset), additional Raman modes appear at higher energies. Theoretical studies for the two-electron QD are also remarkably similar to the experimental observations. Here we have used the value $\hbar\omega_0 = 1.6$ meV for the two-electron QD, which is larger than that for the one electron case [7].

Clearly, the Rashba SO coupling is responsible for additional Raman excitations even for the single-electron system. With an increase (or decrease) of the SO parameter α it is possible to manipulate the amplitudes of these additional excitations. To understand this unique effect we consider the first three one-electron states with total momentum $J_z = 1/2$. Raman excitations with higher amplitude are possible only between the states with the same angular momentum l . Therefore without the SO coupling the transition is only from the ground state to the second excited state. However, the SO coupling mixes all those states and these can be expressed as linear combination of states with different angular momenta l . Therefore, we now have the possibility of Raman transitions from the ground state to both excited states. With a further increase of α the weight of $|1,0\rangle$ state in the first excited state increases, and so does the transition amplitude. With a decrease of α the weight of $|1,0\rangle$ state will

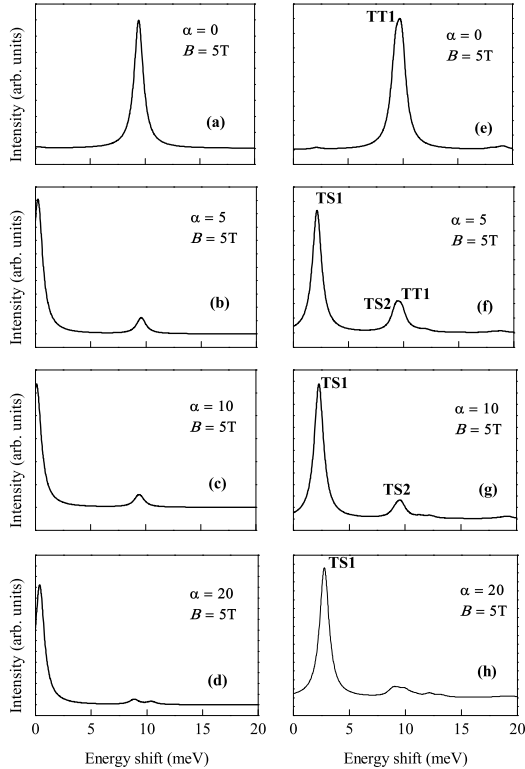


FIG. 4: The same as in Fig. 2, but for a magnetic field of 5 Tesla.

vanish and the additional peak will disappear.

A similar situation is also observed for a two-electron QD (Fig. 2(e)-(h)). Here we see many additional peaks in the observable energy range, in comparison to the case of without the SO coupling. In the latter case and in the absence of the magnetic field the ground two-electron state is singlet with $J_z = 0$ and the Raman transitions are only to singlet excited states with the same total momentum [5]. With the increase of Rashba coupling strength α the SO interaction will again mix the states with different total spins and therefore we can not characterize the states as fully singlet or triplet. All the states must now be presented as superpositions of two-component basis states $|n_1, l_1, \sigma_1\rangle|n_2, l_2, \sigma_2\rangle$. The most important component of the ground state is the singlet state $|0, 0, 1/2\rangle|0, 0, -1/2\rangle$ with weight 70.5% and we can still characterize it as a singlet. Due to the SO mixing, the final states also will have triplet components. As an example, the most important component of the final state in the first peak in Fig. 2(f) is the triplet state $|0, 0, 1/2\rangle|0, -1, 1/2\rangle$ with weight 86.5%. Hence we can call that transition as the singlet-triplet (labelled as ST1) transition. The peaks SS1 and SS2 in Fig. 2(f) are very similar to the peaks for the case without the SO coupling and are essentially singlet-singlet transitions. For these the most important components are $|1, 0, \pm 1/2\rangle|0, 0, \mp 1/2\rangle$ with weight 86.5% and $|2, 0, \pm 1/2\rangle|0, 0, \mp 1/2\rangle$ with weight 69.6% re-

spectively. In Fig. 2(f-h) several singlet-triplet (ST) and singlet-singlet (SS) transitions are visible. With an increase of the SO coupling parameter α the amplitude of the first singlet triplet transition ST1 increases and it becomes the dominant one.

Magnetic field effect – In Figs. 3-4 we present results as in Fig. 2 but for various values of the magnetic field B . According to these results, the magnetic field significantly changes the Raman spectra. For the single-electron case the peaks have become more pronounced and here we again observe the emergence of the transition from the ground state to the first excited state by switching on the SO coupling. These figures indicate that for $\alpha = 20$ the transition amplitude from the ground state to the first excited state is several times bigger than the transition to second excited state compared to the same figure without the magnetic field.

With an increase of the magnetic field, the two-electron ground state changes from singlet to triplet near the field of $B = 1$ Tesla. Therefore without the SO coupling [Fig. 3(e)], the most important component of the ground state is the triplet state $|0, 1, -1/2\rangle|0, 0, -1/2\rangle$ with weight 93% and all possible transitions are triplet-triplet (TT). With an increase of the SO coupling α , we find additional triplet-singlet (TS) and triplet-triplet transitions. For example, the first peak in Fig. 3(f) corresponds to a transition to the final state with the most important component $|0, 0, 1/2\rangle|0, 0, -1/2\rangle$ having weight of 70.7%. Similar to the single-electron case we can tune the amplitudes of the peaks with the magnetic field, and again for $B = 5$ Tesla (Fig. 4) the first additional peak created by the SO coupling becomes dominant. It is however important to note that for weak magnetic fields that peak can be characterized as a singlet-triplet, and for higher values of the magnetic field it becomes triplet-singlet.

To summarize, we have studied the influence of the Rashba spin-orbit coupling on the resonant Raman electronic excitations in one- and two-electron GaAs quantum dots for polarized configuration. We have shown that the SO coupling brings in additional Raman transitions, the amplitudes of which depends on the coupling parameter α . In the case of a two-electron QD, in addition to the usual singlet-singlet and triplet-triplet Raman transitions we also observe the singlet-triplet and triplet-singlet Raman transitions. The external magnetic field can be used to tune the amplitudes of Raman transitions for both one and two-electron systems.

The work was supported by the Canada Research Chairs Program of the Government of Canada and Armenian State Committee of Science (Project No. 11B-1c039). The authors are grateful to Vitorio Pellegrini for providing us with the experimental data of [7].

-
- [1] T. Chakraborty, *Quantum Dots* (North-Holland, Amsterdam, 1999); T. Chakraborty, Comments Condens. Matter Phys. 16, 35 (1992); P.A. Maksym and T. Chakraborty, Phys. Rev. Lett. **65**, 108 (1990).
- [2] U. Merkt, J. Huser, and M. Wagner, Phys. Rev. B **43**, 7320 (1991); D. Pfannkuche and R.R. Gerhardts, *ibid.* **44**, 13132 (1991); D. Pfannkuche, V. Gudmundsson, and P.A. Maksym, *ibid.* **47**, 2244 (1993); D. Pfannkuche, R.R. Gerhardts, P.A. Maksym, and V. Gudmundsson, Physica B **180**, 6 (1993); M. Dineykhon and R.G. Nazimtdinov, Phys. Rev. B **55**, 13707 (1997).
- [3] P.A. Maksym and T. Chakraborty, Phys. Rev. B **45**, 1947 (1992); M. Wagner, U. Merkt, and A.V. Chaplik, *ibid.* **45**, 1951 (1992).
- [4] R.C. Ashoori, H.L. Stormer, J.S. Weiner, L.N. Pfeiffer, S.J. Pearton, K.W. Baldwin, and K.W. West, Phys. Rev. Lett. **68**, 3088 (1992).
- [5] T. Köppen, D. Franz, A. Schramm, Ch. Heyn, D. Heitmann, and T. Kipp, Phys. Rev. Lett., **103**, 037402 (2009).
- [6] C. Schüller, *Inelastic Light scattering of semiconductor nanostructures* (Springer, Heidelberg, 2006).
- [7] A. Singha, V. Pellegrini, A. Pinczuk, L.N. Pfeiffer, K.W. West, M. Rontani, Phys. Rev. Lett., **104**, 246802 (2010).
- [8] C. Schüller, K. Keller, E. Ulrichs, L. Rolf, C. Steinebach, D. Heitmann, and K. Eberl, Phys. Rev. Lett. **80**, 1673 (1998); C.P. Garcia, V. Pellegrini, A. Pinczuk, M. Rontani, G. Goldoni, E. Molinari, B.S. Dennis, L.N. Pfeiffer, and K.W. West, *ibid.*, **95**, 266806 (2005).
- [9] Y.A. Bychkov and E.I. Rashba, J. Phys. C **17**, 6039 (1984).
- [10] T. Dietl, D.D. Awschalom, M. Kaminska, and H. Ohno, (Eds.) *Spintronics* (Elsevier, Amsterdam 2008).
- [11] H. Sanada, T. Sogawa, H. Gotoh, K. Onomitshu, M. Kohda, J. Nitta, and P.V. Santos, Phys. Rev. Lett. **106**, 216602 (2011); S. Takahashi, R.S. Deacon, K. Yoshida, A. Oiwa, K. Shibata, K. Hirakawa, Y. Tokura, and S. Tarucha, *ibid.* **104**, 246801 (2010).
- [12] T. Chakraborty and P. Pietiläinen, Phys. Rev. Lett. **95**, 136603 (2005); P. Pietiläinen and T. Chakraborty, Phys. Rev. B **73**, 155315 (2006); T. Chakraborty and P. Pietiläinen, *ibid.*, **71**, 113305 (2005).
- [13] A. Manaselyan and T. Chakraborty, Europhys. Lett. **88**, 17003 (2009).
- [14] Y. Liu, F. Cheng, X.J. Li, F.M. Peeters, and Kai Chang, Appl. Phys. Lett. **99**, 032102 (2011).
- [15] A. Manaselyan and T. Chakraborty, Europhys. Lett. **94**, 57005(2011).
- [16] A. Delgado, et al., Phys. Rev. B, **79**, 195318 (2009); C.P. Garcia, V. Pellegrini, A. Pinczuk, et al., Physica E, **34**, 304 (2006).